



# Prediction of algal blooms via data-driven machine learning models: an evaluation using data from a well-monitored mesotrophic lake

Shuqi Lin<sup>1,3</sup>, Donald C. Pierson<sup>1</sup>, and Jorrit P. Mesman<sup>1,2</sup>

<sup>1</sup>Erken Laboratory and Limnology Department, Uppsala University, Uppsala, Sweden

<sup>2</sup>Département F.-A. Forel des sciences de l'environnement et de l'eau, Université de Genève, Geneva, Switzerland

<sup>3</sup>Environment and Climate Change Canada, Canada Centre for Inland Waters, Burlington, L7R 4A6 ON, Canada

**Correspondence:** Shuqi Lin (shuqi.lin@ec.gc.ca)

Received: 6 July 2022 – Discussion started: 2 August 2022

Revised: 11 October 2022 – Accepted: 28 November 2022 – Published: 3 January 2023

**Abstract.** With increasing lake monitoring data, data-driven machine learning (ML) models might be able to capture the complex algal bloom dynamics that cannot be completely described in process-based (PB) models. We applied two ML models, the gradient boost regressor (GBR) and long short-term memory (LSTM) network, to predict algal blooms and seasonal changes in algal chlorophyll concentrations (Chl) in a mesotrophic lake. Three predictive workflows were tested, one based solely on available measurements and the others applying a two-step approach, first estimating lake nutrients that have limited observations and then predicting Chl using observed and pre-generated environmental factors. The third workflow was developed using hydrodynamic data derived from a PB model as additional training features in the two-step ML approach. The performance of the ML models was superior to a PB model in predicting nutrients and Chl. The hybrid model further improved the prediction of the timing and magnitude of algal blooms. A data sparsity test based on shuffling the order of training and testing years showed the accuracy of ML models decreased with increasing sample interval, and model performance varied with training–testing year combinations.

2011; Paerl and Huisman, 2008). Moreover, as indicated by Carey et al. (2012) and Huisman et al. (2018), more intense and longer periods of thermal stratification could potentially specifically favour blooms of toxic Cyanobacteria. To better manage and mitigate the effects of algal blooms, methods to forecast their timing and magnitude are needed. However, the factors regulating algal blooms are complex, variable, and site-specific, often involving high-order interactions of environmental factors and biogeochemical processes (Reichwaldt and Ghadouani, 2012; Richardson et al., 2018).

Process-based (PB) models encode our understanding of biogeochemical processes into a framework of numerical formulations, but these are inevitable simplifications that lead to an incomplete description of complex biogeochemical interactions and low level of model confidence (Elliott, 2012). Based on innovative data mining and statistical techniques, data-driven machine learning (ML) models have been applied to identify patterns within observed data (Peretyatko et al., 2012; Mellios et al., 2020), and with the recent proliferation of lake monitoring data (Marcé et al., 2016), ML models have been applied, as an alternative to PB models for bloom prediction (Rousso et al., 2020). Previously applied ML models, including random forest (Nelson et al., 2018), support vector machine (Jimeno-Sáez et al., 2020), and artificial neural network models (Xiao et al., 2017; Recknagel et al., 1998; Wei et al., 2001), can improve predictions of the timing and seasonality of algal Chl pattern, apparently by accounting for complexity that is difficult to encode within the framework of a PB model. However, a downside of data-driven ML models is that they lack the interpretability and generalization found in the explicit structure of the

## 1 Introduction

Harmful algal blooms, which are a serious threat to natural water systems, have been increasing throughout the world (Burford et al., 2020; Watson et al., 2016), primarily as a consequence of both climate change and increased nutrient loading from anthropogenic activities (Brookes and Carey,

PB model. In recent years, the process-guided deep learning (PGDL) model has emerged and has been applied to water temperature (Jia et al., 2019; Read et al., 2019) and water quality (Hanson et al., 2020) simulations, which explicitly combine well-defined physical theories into the training of ML models, enhancing their interpretability. While this approach has achieved promising results, it is difficult to apply it to phytoplankton dynamics due to numerous nonlinear interactions within the biogeochemical cycles and the difficulty in defining a measurable processes or mass balances that can be used as a physical constraint on knowledge-guided decisions. Also, the sparsity of lake water quality (e.g. nutrients and Chl concentration) observations can limit the application of ML models in algal bloom modelling (Rousso et al., 2020).

In this study, our objectives are to (1) apply the ML models to predict algal bloom in a well-monitored mesotrophic lake, (2) evaluate model performance and assess model uncertainties, and (3) explore the approaches to improve the model performance and widen the model applications. We first tested the ability of ML models in predicting algal Chl concentrations via available environmental factors, including observed lake nutrient data, and then proposed a two-step ML approach for predicting algal dynamics that first estimates lake nutrient concentrations which often have limited observations and secondly predicts variations in algal Chl using these pre-generated nutrient concentrations combined with other observed environmental factors that are collected at higher frequency. We also tested a simple hybrid model architecture that, by adding hydrodynamic features derived from the PB model into the training features of the two-step ML approach, allowed us to include additional information describing physical lake processes expected to affect variations in algal growth and succession in the machine learning prediction.

We applied the above workflows to predict changing Chl concentration, as a proxy for the occurrence of algal blooms, via the gradient boost regressor (GBR) and long short-term memory network (LSTM). Two shuffling year tests were conducted. One assessed the uncertainty of ML models in predicting Chl during the same 2-year period, and the other evaluated the sensitivity of ML accuracy to various training–testing year combinations and lake nutrient sampling intervals. Model performance and potential applications in algal bloom forecasting are discussed.

## 2 Methods

### 2.1 Study site

The study site, Lake Erken, is a mesotrophic lake located in east-central Sweden that has a surface area of 24 km<sup>2</sup>, a maximum depth of 21 m, and an average retention time of 7 years. The lake is dimictic, with seasonal stratification commonly

beginning in May–June and ending in August–September. The onset of ice cover usually begins in December–February, and the loss of ice occurs in March–April (Persson and Jones, 2008). Located near the Baltic coast, Lake Erken is wind-exposed and susceptible to periodic wind-induced turbulent mixing.

Changes in algal Chl in Lake Erken have a typical seasonal pattern, with spring and summer peaks in concentration (Pettersson et al., 2003). Spring blooms are dominated by dinoflagellates and diatoms (Pettersson, 1985) and initiated by overwinter species from the last autumn (Yang et al., 2016). Cyanobacteria dominate summer peaks in Chl, given that they can optimize their vertical position with regard to nutrients and light (Paerl, 1988; Pierson et al., 1992).

### 2.2 Data

Lake Erken has a long-running automated monitoring programme that provides hourly meteorological data, water temperature profiles between 0.5 and 15 m at 0.5 m intervals, and the flow from the inflow and outflow (Fig. 1). A manual sampling programme collects samples during ice-free time at 5–7 d intervals for all major nutrient concentrations (e.g. NO<sub>x</sub>, NH<sub>4</sub>, PO<sub>4</sub>, total P, and Si, etc.), dissolved oxygen (O<sub>2</sub>), and Chl concentration. The timing of the onset and loss of ice cover are also monitored yearly by the lab. More detailed information on the sampling programme is in the Supplement (see Sect. S1) and Moras et al. (2019).

### 2.3 Modelling methods

#### 2.3.1 Process-based (PB) lake model

In this study, a PB hydrodynamic lake model, GOTM (General Ocean Turbulence Model; Burchard et al., 1999), was used to generate water temperature profiles and other hydrodynamic metrics. GOTM also served as the foundation of water quality simulations made with the SELMAPROT-BAS model (Mesman et al., 2022) that is coupled to GOTM through the Framework for Aquatic Biogeochemical Models (FABM; Bruggeman and Bolding, 2014).

#### 2.3.2 Data-driven machine learning (ML) models

Tree models have been widely applied in modelling phytoplankton dynamics in freshwater systems (Harris and Graham, 2017; Fornarelli et al., 2013; Rousso et al., 2020). The gradient boosting regressor (GBR) is one of these tree models, iteratively generating an ensemble of estimator trees with each tree improving upon the performance of the previous. Details about the GBR model can be found in Friedman (2001). The hyperparameters in GBR are optimized via the *RandomizedSearchCV* function within the Scikit-Learn library. The loss function of model is chosen as “huber”, which is a combination of the squared error and absolute error of regression. Since the target variable in our research Chl

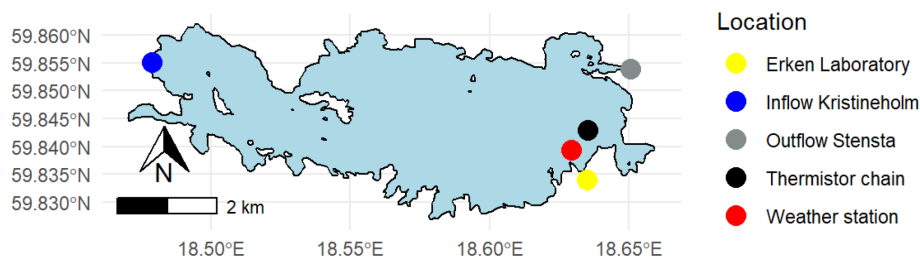


**Figure 1.** Map of Lake Erken. The locations of the monitoring systems are shown.

concentration has peak values during algal blooms, which could be regarded as outliers, the huber loss function is more robust and gives greater weight to peak values than the mean squared error function.

The long short-term memory (LSTM) network is part of a class of deep learning architectures, called recurrent neural networks (RNNs), built for sequential and time series modelling (Hochreiter and Schmidhuber, 1997). The core concepts of LSTM are the cell and hidden states and its three gates (input gate, forget gate, and output gate; see Fig. S2 in the Supplement). Essentially, the LSTM model defines a transition relationship for a hidden representation through a LSTM cell which combines the input features at each time step with the inherited information from previous time steps. This architecture is suitable for extracting information from sequential data (Rahmani et al., 2021; Read et al., 2019). The hyperparameter settings in LSTM can be found in the Supplement (see Sect. S2).

Compared to the GBR model, LSTM has more complex model architectures, carrying the “memory” from the previous time steps. In this study, the GBR and LSTM were applied, respectively, to assess the performance of ML models with and without memory. Both ML models are built in Python using the Scikit-Learn (<https://scikit-learn.org/stable/>, last access: 19 September 2022) and TensorFlow (<https://www.tensorflow.org/>, last access: 19 September 2022) libraries.

## 2.4 Design of predictive workflows and shuffling year data sparsity tests

In this study, we tested three workflows using a dataset split for training (years 2004–2016) and testing (years 2017–2020). In all three workflows, a 5-fold cross-validation using the training dataset was used to optimize the hyperparameters in the ML models. Workflow 1 directly predicts Chl concentration based on available environmental observations (Table 1). The training and testing datasets were limited by the frequency of lake nutrient observations, which resulted in 5–7 d gaps between data points. The time step of LSTM was set to 1; that is, the environmental factors on the target date and previous observation date, which may be 5–7 d ago, were used to train the model and make predictions.

In workflow 2 and 3, a two-step approach was applied (Table 1). Daily measurements of physical factors were used to pre-generate daily variations in lake nutrients via separate ML models, and the ML models were trained at a daily time step using the measured environmental factors and pre-generated nutrient concentrations. The time step of LSTM was then set to 7 d.

In workflow 3, three hydrodynamic features, i.e. mixing layer depth ( $z_e$ ), Wedderburn number ( $Wn$ ), and the seasonal thermocline depth (thermD), derived from the GOTM model were regarded as daily training features in the two-step ML approach. The definitions and calculations of these features are explained in the next section, Sect. 2.5, “Feature selection and processing for ML models”, and the Supplement (Sect. S3).

Following the two-step approach and using workflow 3, we set up two tests. (1) To assess the uncertainty induced by variations in the data used to train the ML models, we shuffled the training years, randomly taking 13 years out of the 2004–2018 dataset 30 times, and tested the model predictions of Chl during 2019–2020. And, (2) to test if the workflow could be used for other water systems which may have less frequent lake nutrient monitoring data, we conducted a data sparsity test that evaluated the sensitivity of models to the lake nutrient and Chl sampling interval. For this test the lake nutrient and Chl concentration observations in the training dataset were downsampled to a 7, 14, 21, 28, and 35 d sampling interval. Then for each sampling interval using the 2004–2020 dataset, Chl was predicted for different consecutive 4-year periods when the ML models were trained by the remaining 13 years of data. Data shuffling was conducted 13 times so that every 4-year period in our dataset was tested.

## 2.5 Feature selection and processing for ML models

The feature selection process is based on some a priori knowledge of the underlying phenomena related to algal blooms. All workflows made use of the daily automated monitoring data. In addition, the temperature difference ( $\Delta T$ ) between surface water (averaged over the upper 3 m) and bottom water (15 m) was also used to represent the thermal structure of the lake, and the duration of ice cover in

**Table 1.** List of training features and target variables in each workflow. Stars (\*) indicate training features, circles (o) indicate target variables, and squares ( $\square$ ) indicate the variables are the target variables in step 1 used to daily produce a training feature for use in step 2. The order of nutrient model sequence is from the top to bottom based on its position in the table ( $\text{NO}_x$  to Si).

Variables	Sample interval	Workflow 1	Workflow 2		Workflow 3	
			Step 1	Step 2	Step 1	Step 2
Inflow	Daily	*	*	*	*	*
Meteorological data (air temperature, wind speed, short-wave radiation, precipitation, humidity, and cloud cover)	Daily	*	*	*	*	*
$\Delta T$	Daily	*	*	*	*	*
Ice duration	Daily	*	*	*	*	*
Days from ice-off date	Daily	*	*	*	*	*
$z_e$	Daily				*	*
$Wn$	Daily				*	*
thermD	Daily				*	*
$\text{NO}_x$	1–2 weeks	*	$\square$	*	$\square$	*
$\text{O}_2$	1–2 weeks	*	$\square$	*	$\square$	*
$\text{PO}_4$	1–2 weeks	*	$\square$	*	$\square$	*
Total P	1–2 weeks	*	$\square$	*	$\square$	*
$\text{NH}_4$	1–2 weeks	*	$\square$	*	$\square$	*
Si	1–2 weeks	*	$\square$	*	$\square$	*
Chl	1–2 weeks	o		o		o

the previous winter and the number of days from ice-off date were used.

In workflow 2 and 3 nutrients are predicted sequentially, with each pre-generated nutrient prediction included in the training data of the next nutrient prediction (Table 1). Workflow 3 added  $z_e$ , computed using the GOTM-simulated vertical eddy diffusivity ( $K_z$ ) profiles; thermD, estimated using Lake Analyzer (Read et al., 2011) based on GOTM-simulated temperature profiles; and  $Wn$ , a dimensionless parameter measuring the balance between wind stress and the pressure gradient resulting from the slope of the interface (see Sect. S3), as additional daily training features.

## 2.6 Evaluating metrics

Model performance was evaluated by comparing the simulated and measured Chl concentrations and by calculating the mean absolute error (MAE), root mean square error (RMSE), and correlation coefficient ( $R^2$ ). To evaluate the accuracy of the model in detecting the onset of an algal bloom, we calculated a confusion matrix in workflows 2 and 3, where the observations were linearly interpolated to daily values, and predicted daily Chl concentration were smoothed with a 7 d

rolling mean. Using these data, the onset of a bloom was categorized as occurring when the daily change of Chl ( $\Delta\text{Chl}$ ) exceeded a threshold,  $0.35 \text{ mg m}^{-3} \text{ d}^{-1}$ . This works well in Lake Erken where Chl concentrations are frequently monitored (near weekly), and the linear interpolation can be expected to be reasonably representative of the Chl concentrations between measured samples. Considering the randomization in the ML models, we also add a 3 d window on the bloom onset prediction; that is, we considered the prediction of a bloom valid if the measured data suggested a bloom the day before or after the simulated onset. We used the true positive rate (TPR), false positive rate (FPR), and modified accuracy (kappa), which considers the possibility of the agreement occurring by chance (McHugh, 2012), to identify the potential of ML models to correctly capture the algal bloom onset (see Table S1). A model with 100 % TPR, 0 % FPR, and 100 % kappa would constitute a perfect fit.

### 3 Results

#### 3.1 Workflow 1: direct prediction based on observations

In workflow 1, both the GBR and LSTM clearly reproduced spring and summer blooms (Fig. 2a) but underestimated the intensity of blooms (Fig. 2a, b). Neither ML model captured the extraordinarily high Chl ( $\sim 15\text{--}30\text{ mg m}^{-3}$ ) in the summer of 2019. Although the abnormal summer bloom in 2019 could contribute to the higher RMSE and MAE in the testing dataset than the mean values in the training dataset, the cross-validation on the training dataset (see Table S2) shows what appears possibly to be an overfitting issue in both models. The achieved accuracy of models is attributed to the daily availability of physical inputs and the fact that in Lake Erken water samples are collected frequently at 5–7 d intervals. Workflow 1 may be most valuable in reconstructing previous variations in algal Chl, filling the gaps between measured Chl observations and feature importance ranking (see Fig. S4). But when using this workflow, future forecasts will be limited by the absence of future nutrient data.

#### 3.2 Workflow 2: two-step ML models based on pre-generated daily nutrients and observed physical factors

As in workflow 1, both ML models in workflow 2 had poor fit in the summer of 2019 and suffered from overfitting leading to higher MAE and RMSE and lower  $R^2$  in testing datasets than training datasets (see Table S2).

Overall, both the GBR and LSTM showed slightly higher MAE ( $4.22\text{ mg m}^{-3}$  vs.  $3.87\text{ mg m}^{-3}$ ) and RMSE ( $6.27\text{ mg m}^{-3}$  vs.  $6.00\text{ mg m}^{-3}$ ) when compared to workflow 1 (Table 2). But they also showed improved performance in terms of capturing the peak values of Chl during spring blooms (Figs. 2, S5). Both workflows outperformed the SELMAPROTBAS PB model in simulating concentrations of lake nutrients (see Fig. S6). The ML models were more accurate in predicting the low values of  $\text{NO}_x$  and peak values of  $\text{PO}_4$  and total P. However, both ML models and the PB model failed in predicting the extremely high values of measured lake nutrients, such as the autumn peak of  $\text{NH}_4$  in 2017 (Fig. S6e) and the spring peak of  $\text{O}_2$  in 2018 (Fig. S6c). Thus, higher workflow 2 MAE and RMSE (Table 2) are presumably due to the inaccuracies in the pre-generated nutrient training data, but the improved daily predictions that better capture the bloom events overshadow these flaws.

#### 3.3 Workflow 3: based on workflow 2 and including hydrodynamic training features derived from the GOTM model

Including hydrodynamic training information in workflow 3 did not significantly improve lake nutrient predictions compared to workflow 2 (see Fig. S6), and when using workflow

3 both ML models showed comparable performance in Chl predictions compared to workflow 1. However, the predictions of the spring bloom in all years improved compared to workflows 1 and 2, in terms of the magnitude and timing of the spring bloom (Fig. 2e). This was the case in 2019–2020 (Fig. 2a), which was an abnormally warm winter with only 5 d ice cover and had an unusually early spring algal bloom. Both the GBR and LSTM in workflows 2 and 3 did not capture the extremely intensive bloom (with peak values close to  $30\text{ mg m}^{-3}$ ) in summer of 2019, and neither did the PB model.

Furthermore, adding hydrodynamic features derived from the PB model improved predictions of the onset of algal blooms (Figs. 2e and 4), with the overall TPR increasing by 15 % and 5 % and FPR increasing around 5 % and 3 % in the GBR and LSTM models, respectively. Compared with the PB model, which showed lower TPR (15 %) and FPR (6 %), ML models are more likely to predict algal bloom at the correct time. The optimal TPR was from LSTM in workflow 3, which could detect the onset of algal blooms with TPR closed to 50 %. However, the concomitant higher FPRs indicating an incorrect warning of algal bloom is also more likely to occur in the ML models, since the PB model is more likely to miss the bloom entirely. The kappa values of both ML models and the PB model are close to 80 %, showing that all models simulated the entire period (blooms and the periods between blooms) to a moderate–strong level (McHugh, 2012).

#### 3.4 Effects of shuffling training years on 2019–2020 predictions

The results presented so far are based on a typical strategy of training ML models for a historical period, in this case 2004–2016, and then accessing model performance in a second period between 2017–2020. The accuracies of the model predictions were to some extent related to the range and variability in the training data. To evaluate the importance of this, we randomly removed 2 years from a 2004–2018 training dataset and made 30 different predictions of Chl during 2019–2020 when the models had difficulties predicting spring and summer blooms (Fig. 5). When trained with the various shuffled combinations, both ML models were capable of reproducing the seasonal variations in algal Chl with a 4.5 % and 5.8 % coefficient of variation (CV) in MAE and a 24.0 % and 16.4 % CV in TPR of GBR and LSTM, respectively (see Table S3 in the Supplement). This provides an indication of the uncertainty that may arise as a consequence of differences in the training datasets used for in our workflows. And, it also shows that even a relatively long training period of 13 years can not totally capture the system behaviour in such a way as to lead to nearly similar bloom predictions.

Although none of the model runs captured the intensive summer bloom in 2019, the spring bloom in both years was

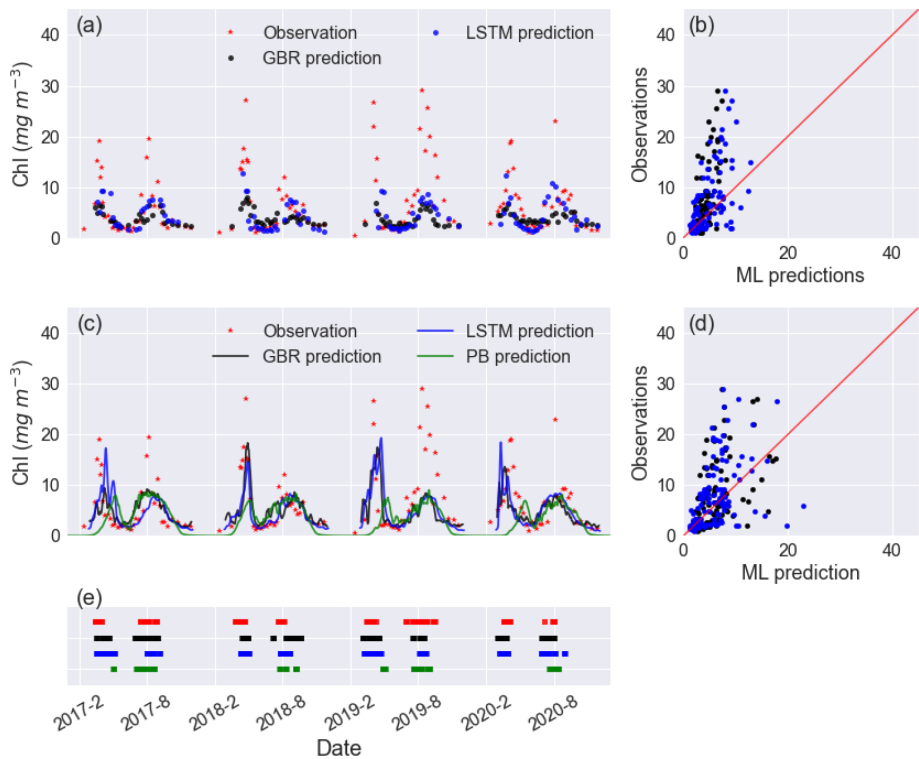


**Figure 2.** Time series of observed and predicted Chl from GBR and LSTM models in (a) workflow 1 and (c) workflow 3, and the corresponding scatter plots of observations vs ML predictions of Chl in workflow 1 and workflow 3 are shown in panels (b) and (d), with the black and blue dots and lines representing the predictions from GBR and LSTM, respectively. Panel (e) shows the observed and predicted algal bloom onsets in 2017–2020 using the same colour coding as the previous panels. Results from the PB model simulation in Mesman et al. (2022) are also shown in (c) and (e).

**Table 2.** Comparisons of model performance during the testing period based on RMSE, MAE, and  $R^2$ . The unit of Chl is milligrams per cubic metre ( $\text{mg m}^{-3}$ ). In bold are the best fits of each statistical metric. For comparison of training and testing periods, see Table S2.

Model	PB	ML-workflow 1		ML-workflow 2		ML-workflow 3	
		GBR	LSTM	GBR	LSTM	GBR	LSTM
RMSE	7.18	5.77	<b>5.64</b>	6.27	6.00	5.94	5.81
MAE	4.77	<b>3.55</b>	3.58	4.22	3.87	3.99	3.71
$R^2$	−0.25	0.13	<b>0.20</b>	0.05	0.13	0.14	0.18

well represented, especially by LSTM, in terms of timing and magnitude.

Despite comparable RMSE and MAE in LSTM and the GBR (Fig. 4c), both higher TPRs (with median of 60 %) and FPRs (with median of 18 %) in LSTM indicate that the LSTM model was more aggressive in making algal bloom predictions. The GBR model’s apparent advantage in FPRs (with median 10 %) is largely the result of it making a lower number of bloom predictions since the low concentrations between spring and summer blooms in 2020 were not well represented (Fig. 4b).

3.5 Shuffling year data sparsity test

To examine the possible use of workflow 3 when data are less frequently available, lake nutrient and Chl data were down-sampled so that the effects of sampling frequency on model predictions could be evaluated. Each downsampled dataset was also rearranged into 13 different 13-year training periods and 4-year testing periods. The variability in predictions provided a measure of model performance and uncertainty. Figure 5 shows the uncertainty in model predictions as a consequence of the chosen sampling intervals.

The MAEs and RMSEs of both GBR and LSTM models tended to increase with the longer sample intervals. The median MAE was always slightly higher for the LSTM model,



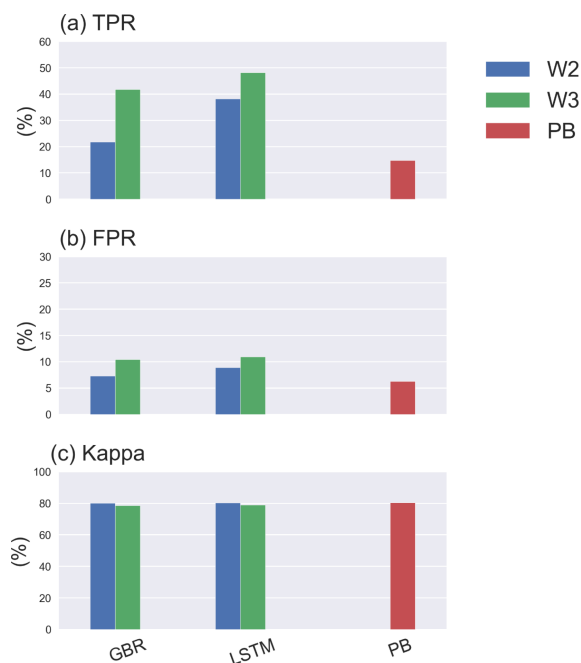


**Figure 3.** TPR, FPR, and kappa of GBR and LSTM models in workflow 2, 3, and the PB model.

except when trained with the original dataset (Fig. 5a). While our initial evaluation of TPR using 2017–2020 as the testing period and 2004–2016 as the training period suggested the LSTM model was more accurate in turns of detection of algal bloom onsets (Fig. 3), Fig. 5c showed the median TPR of GBR model calculated by the shuffling year test was over 50 %, higher than that found when using the original testing and training periods. This can be explained by the fact that the 2017–2020 testing period as in Fig. 3 and shown as large points in Fig. 5 was unusually difficult for the GBR to simulate. Consequently, even though the GBR model usually performs better in the shuffled data test in Fig. 5, Fig. 3, which show the results of the 2017–2020 testing period, presented the opposite result. This illustrates the importance of the sequence of training and testing years for evaluating model performance.

For the first three sampling intervals the GBR model clearly had better TPR values than the LSTM model. The median TPRs of GBR model started to drop below 30 % once the sample interval reached 21 d. For LSTM, medium TPRs remained lower than 30 %, for all sampling intervals, but also showed a much wider range of variability (Table S4) dependent on the training and tested datasets used. In general, both models performed best at the original and 7 d sampling interval but then showed slightly worse performance that was consistent up to a sample interval of 21 d. In terms of the errors evaluated over the entire 4-year testing period (Fig. 5a, b) the GBR model had lower errors and, therefore, better predicted the seasonal variations of Chl concentration. The time

series comparison of observed and predicted Chl from this shuffling year data sparsity test can be found in the Supplement (Figs. S7–S9).

## 4 Discussion

### 4.1 Performance of ML models

In three workflows, the ML models successfully reproduced the Chl seasonal patterns, capturing the spring and summer bloom events, with lower averaged RMSEs and MAEs than a PB model simulation that was previously calibrated for Lake Erken. And in all three workflows, LSTM model always showed slightly lower RMSE and MAE and higher  $R^2$  in predicting Chl concentrations than the GBR model and higher TPR in detecting the onset of algal bloom events. Workflow 1, which predicted Chl based on all available environmental factors including lake nutrient observations, showed that both ML models can reproduce the seasonal dynamics of algal Chl with promising accuracy ( $MAE = 3.55$  and  $3.58 \text{ mg m}^{-3}$ ,  $RMSE = 5.77$  and  $5.64 \text{ mg m}^{-3}$ , and  $R^2 = 0.13$  and  $0.20$ , for GBR and LSTM, respectively) via the direct input of available environmental observations. These ML models can be applied to reconstruct past patterns of algal Chl, fill the gaps between measured Chl observations, and interpret the mechanisms that drive phytoplankton dynamics. Workflows 2 and 3 adopted a two-step approach, first using separate ML models to estimating daily changes in lake nutrient concentration and in Workflow 3 also including PB model derived physical factors as training features of the algal ML model. These two workflows allowed for daily predictions of changes in algal Chl concentration using both observations and pre-generated lake nutrient concentrations at a consistent daily time step, and at only a minor decrease in performance compared to workflow 1, workflow 2 and 3 demonstrated a wider potential range of applications (e.g. interpolation, reconstruct historical data, and algal bloom forecast) via making daily forecasts with less-than-daily measured nutrient observations.

The one clear failure of both the ML- and PB-based model predictions was that during July–August 2019, Chl concentrations in integrated samples collected between the surface and 6–12 m exceeded  $20 \text{ mg m}^{-3}$  over a 5-week period. Neither the PB model nor ML models captured this unusually persistent bloom (Figs. 2, S3). At this time the phytoplankton were dominated by the Cyanobacteria *Gloeotrichia* and *Anabaena*, that form a resting akinete life stage at the end of their yearly bloom, which can initiate the following year's bloom as they are transformed to vegetative cells that migrate from the sediment to the upper water column. We hypothesize that the large summer bloom in 2019 was the result of unusually large recruitment of akinetes in this year (Karlsson-Elfgren et al., 2005, 2004). The life cycle of Cyanobacteria is not a process included in the PB model (but see Hense and Beckmann, 2006, and Jöhnk et al., 2011), so

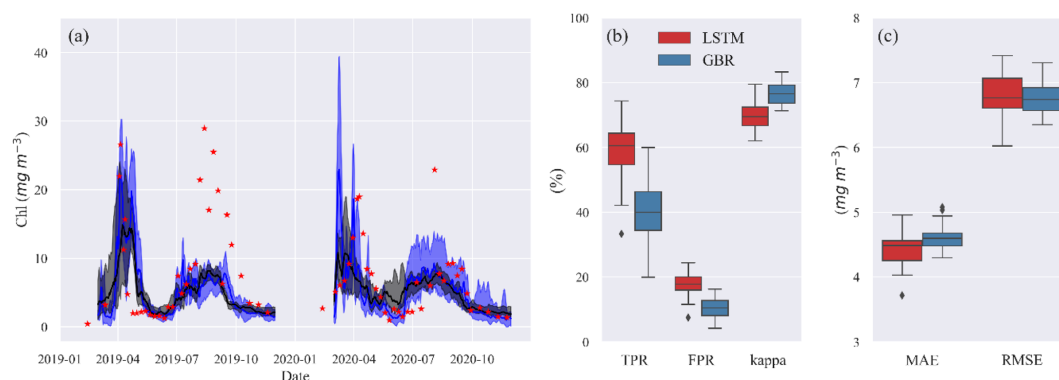


**Figure 4.** (a) Time series of observed (red stars) and predicted Chl from GBR (black) and LSTM (blue) models in the shuffling training year test. The shades represent the range between minimum and maximum prediction, and the solid lines represent the median prediction. Panel (b) shows the box plot of TPR, FPR, and kappa, and panel (c) shows the box plot of MAE and RMSE of both models in the shuffling training year test.

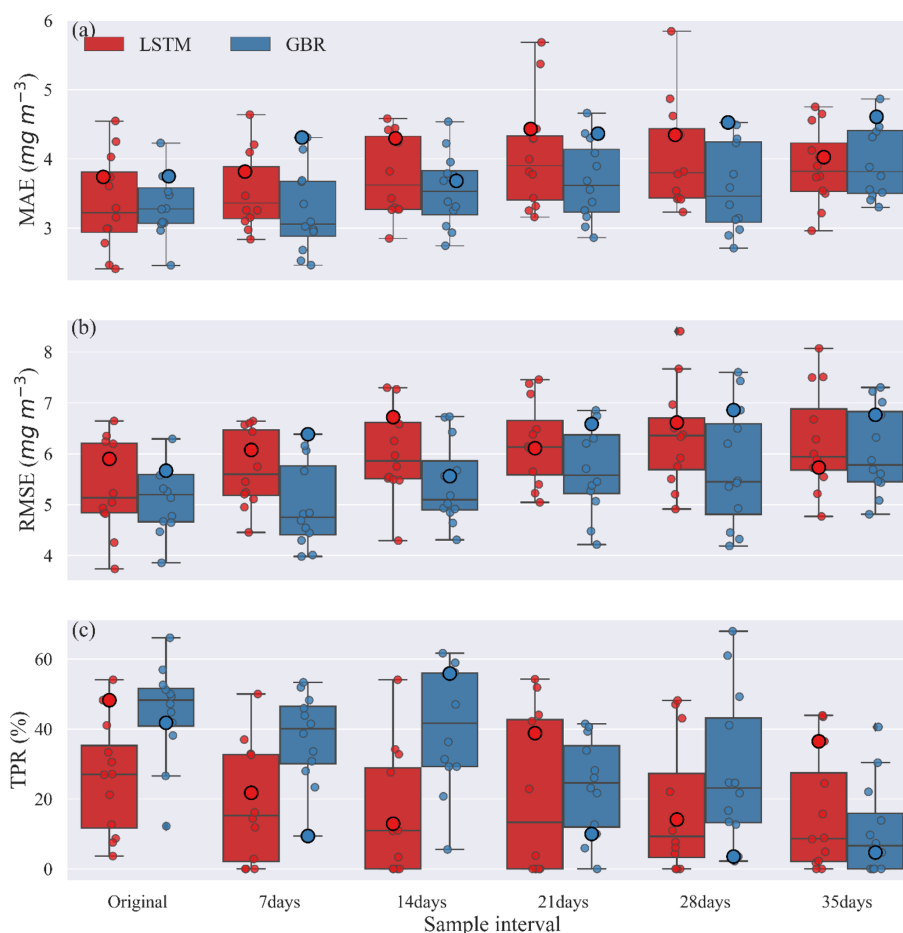


**Figure 5.** Comparisons of (a) MAE, (b) RMSE, and (c) TPR between GBR and LSTM during the testing period created under various sample intervals. Circles along the box show the result from the testing period of all shuffled training–testing year combinations, and the bigger circles represent 2004–2016 training and 2017–2020 testing year combination, as used in Fig. 2.



increased recruitment of akinetes could explain the underestimation of the 2019 summer bloom. Even the LSTM algorithms could not account for previous conditions so far back in time as to affect the formation and deposition of Cyanobacteria akinetes (this may require the memory of the last ice-free season). The consequent poor fit of summer bloom in 2019 partially led to the higher MAE and RMSE in the testing dataset compared to the training dataset in all three workflows, in both GBR and LSTM models.

Warm winters can initiate a chain of events, i.e. shortening the ice cover duration, extending spring circulation, affecting nutrient availability, and causing an earlier spring bloom (Adrian et al., 2006; Yang et al., 2016). According to the ice record in Lake Erken (see Fig. S1), in 2020, the lake was covered by very thin ice for only 5 d, which is the shortest duration since observations were first recorded in 1954. The spring bloom in 2020 did occur earlier than other years (see Fig. S3), and both ML models which considered the timing of lake ice show fairly good performance in predicting the timing and magnitude of this abnormally early spring bloom (Figs. 2, 5)

#### 4.1.1 Performance of hybrid PB ML models

One-dimensional PB hydrodynamic models can accurately simulate both water temperature profiles and other hydrodynamic features in Lake Erken using the same forcing data that are commonly input to ML models. The hybrid model structure tested here provides a richer set of input data, leading to more accurate ML predictions of algal Chl at little additional computational cost or data requirements. Using data from the hydrothermal PB model allowed for the seasonal deepening of the thermocline and variations in the surface mixing layer depth and upwelling events, represented by  $W_n$ , to be encoded into the ML algorithms. These factors can affect the underwater light climate, the internal loading of phosphorus, and the transport of resting Cyanobacteria colonies from the hypolimnion into the epilimnion, favouring summer blooms of Cyanobacteria (Pierson et al., 1992; Pettersson, 1998). The inclusion of these factors did increase the accuracy of the ML models, especially in the case of unusual environmental conditions (e.g. spring of 2020, Figs. 2, 5) that did not frequently occur in the remaining meteorological, hydrological, and biogeochemical training data.

#### 4.1.2 Prediction of bloom timing

For the purposes of water management, it may be most important to first predict the potential occurrence of a bloom and then once underway improve predictions of its magnitude. The best model performance in predicting the timing of algal blooms was obtained after adding hydrodynamic features derived from a PB model in workflow 3, with TPR above 45 % in detecting the onset of algal bloom during

2017–2020 and a modified accuracy (kappa) around 80 %, indicating a moderate–strong level of prediction.

Based on our shuffling year tests of bloom timing, the GBR model showed relatively higher median TPRs than the LSTM model for sample intervals less than 1 month. However, in some training and testing year combinations, TPRs are close to 0 % (Fig. 5), and CVs of the TPRs are highly variable, even at the original sample interval, being over 30 % for GBR and over 60 % for LSTM, indicating that the correct detection of algal blooms in both models is highly dependent on the years used to train the models. Thus, while the ML models can be better than the PB models at predicting the onset of algal blooms, they still may not be good enough for operational forecasting. The resulting variability provided a more accurate estimate of the model performance at each down-sampled data interval and showed that increasing sample interval led to reduced performance for both ML models, in terms of MAE, RMSE, and the CV of TPR. These tests also highlighted that the performance of both ML models, especially LSTM, varied with the sampled history of events in the training period for evaluating a specific pattern of change in the testing period. We suggest that testing strategies similar to the shuffle methods used in this study are needed to accurately evaluate the expected accuracy of ML models when applied to any given site. The estimated uncertainty in shuffling training year tests (Fig. 4) and shuffling training–testing year tests (Fig. 5) can be used to better represent the uncertainty of ML derived forecasts.

#### 4.2 Future applications in short-term forecasts and water management

To reach the goal of incorporating ML models into operational forecasts either for short-term management support or longer-term evaluation and planning, two steps must occur. First the ML model must be developed, trained, and evaluated on the water body of interest due to the unique physical characteristics and water quality dynamics in different systems. Secondly, future forcing data for the model must be obtained and integrated into a workflow that makes the future predictions. In regards to the second point, a lack of frequent water monitoring (Stanley et al., 2019) is a major deterrence to applying ML models to many lakes. The data sparsity test (Fig. 5) showed that, at least for Lake Erken, the ML models can still detect the seasonal algal dynamics even for sample intervals approaching 1 month (Figs. S7–S9). If this result holds for other lakes, the use of the two-step ML workflow could offer a method of forecasting seasonal variations in algal Chl, even in lakes with relatively infrequent nutrient monitoring but higher frequency meteorological and hydrological data.

The hybrid PB/ML models have the potential to provide reasonably accurate and timely short-term algal bloom forecasts, working as part of an early-warning system for the water resource management (Baracchini et al., 2020), and

clearly have the ability to predict border seasonal variations in algal Chl concentration. However, since a large number of water temperature and water quality samples are required for ML training, and since our results only apply to one well-studied lake, obtaining more datasets to test and evaluate the workflows developed here is necessary. Monitoring networks (e.g. Global Lake Ecological Observatory Network, GLEON; <https://gleon.org/>, last access: 19 September 2022), could provide the data to allow more extensive testing and application of hybrid PB/ML models, and we are presently working in the GLEON network to test the methods developed in this paper on many other lakes.

**Code availability.** Model version 1.0 has been archived in Zenodo under <https://doi.org/10.5281/zenodo.7149563> (Lin, 2022) and is available at [https://github.com/Shuqi-Lin/Erken\\_Algal\\_Bloom\\_Machine\\_Learning\\_Model.git](https://github.com/Shuqi-Lin/Erken_Algal_Bloom_Machine_Learning_Model.git) (last access: 21 December 2022).

**Data availability.** All data from this study have been archived with the code in Zenodo under <https://doi.org/10.5281/zenodo.7149563> (Lin, 2022) in the “training data” folder. Here we also provide the model forcing data in the format used in the machine learning models. Data collected by the Erken laboratory in the archived format used by the Swedish Infrastructure for Ecosystem Science (SITES) are available from the SITES data archive at [https://hdl.handle.net/11676.1/qZYc4CMTOyxgvjv\\_gTAW08SO](https://hdl.handle.net/11676.1/qZYc4CMTOyxgvjv_gTAW08SO) (Erken Laboratory, 2022).

**Supplement.** The supplement related to this article is available online at: <https://doi.org/10.5194/gmd-16-35-2023-supplement>.

**Author contributions.** The concept of ML model workflow was designed by SL and DCP. SL developed the ML model code and performed the simulations. JPM conducted the PB model simulations. SL wrote the manuscript with contributions from DCP and JPM.

**Competing interests.** The contact author has declared that none of the authors has any competing interests.

**Disclaimer.** Publisher’s note: Copernicus Publications remains neutral with regard to jurisdictional claims in published maps and institutional affiliations.

**Acknowledgements.** Shuqi Lin and this study are funded by the EU and FORMAS project 2018-02771, in the frame of the collaborative international Consortium BLOOWATER (<https://www.bloowater.eu/>, last access: 19 September 2022), financed under the ERA-NET WaterWorks2017 Cofounded Call. This ERA-NET is an integral part of the 2018 Joint Activities developed by the Water Challenges for a Changing World Joint Program Initiative (Water

JPI). Jorrit P. Mesman was funded by the European Union’s Horizon 2020 Research and Innovation Programme under grant agreement nos. 722518 (MANTEL ITN) and 101017861 (SMARTLAGOON). This study has been made possible by the Swedish Infrastructure for Ecosystem Science (SITES), in this case by data from the Erken Laboratory of Uppsala University. SITES receives funding through the Swedish Research Council under grant no. 2017-00635.

**Financial support.** This research has been supported by the Svenska Forskningsrådet Formas (grant no. 2018-02771).

**Review statement.** This paper was edited by Le Yu and reviewed by two anonymous referees.

## References

- Adrian, R., Wilhelm, S., and Gerten, D.: Life-history traits of lake plankton species may govern their phenological response to climate warming, *Glob. Change Biol.*, 12, 652–661, <https://doi.org/10.1111/j.1365-2486.2006.01125.x>, 2006.
- Baracchini, T., Wüest, A., and Bouffard, D.: MeteoLakes: An operational online three-dimensional forecasting platform for lake hydrodynamics, *Water Res.*, 172, 115529, <https://doi.org/10.1016/j.watres.2020.115529>, 2020.
- Brookes, J. D. and Carey, C. C.: Resilience to Blooms, *Science*, 334, 46–47, <https://doi.org/10.1126/science.1207349>, 2011.
- Bruggeman, J. and Bolding, K.: A general framework for aquatic biogeochemical models, *Environ. Modell. Softw.*, 61, 249–265, <https://doi.org/10.1016/j.envsoft.2014.04.002>, 2014.
- Burchard, H., Bolding, K., and Villareal, M. R.: GOTM, a General Ocean Turbulence Model: Theory, Implementation and Test Cases, European Commission, Joint Research Centre, Space Applications Institute, 103, [https://books.google.be/books/about/GOTM\\_a\\_General\\_Ocean\\_Turbulence\\_Model.html?id=zsJUHAACAAJ&redir\\_esc=y](https://books.google.be/books/about/GOTM_a_General_Ocean_Turbulence_Model.html?id=zsJUHAACAAJ&redir_esc=y) (last access: 19 September 2022), 1999.
- Burford, M. A., Carey, C. C., Hamilton, D. P., Huisman, J., Paerl, H. W., Wood, S. A., and Wulff, A.: Perspective: Advancing the research agenda for improving understanding of cyanobacteria in a future of global change, *Harmful Algae*, 91, 101601, <https://doi.org/10.1016/j.hal.2019.04.004>, 2020.
- Carey, C. C., Ibelings, B. W., Hoffmann, E. P., Hamilton, D. P., and Brookes, J. D.: Eco-physiological adaptations that favour freshwater cyanobacteria in a changing climate, *Water Res.*, 46, 1394–1407, <https://doi.org/10.1016/j.watres.2011.12.016>, 2012.
- Elliott, J. A.: Is the future blue-green? A review of the current model predictions of how climate change could affect pelagic freshwater cyanobacteria, *Water Res.*, 46, 1364–1371, <https://doi.org/10.1016/j.watres.2011.12.018>, 2012.
- Erken Laboratory: Meteorological data from Erken, Malma island, 1988-10-12–2021-12-31, Swedish Infrastructure for Ecosystem Science (SITES) [data set], [https://hdl.handle.net/11676.1/qZYc4CMTOyxgvjv\\_gTAW08SO](https://hdl.handle.net/11676.1/qZYc4CMTOyxgvjv_gTAW08SO), last access: 19 September 2022.
- Fornarelli, R., Galelli, S., Castelletti, A., Antenucci, J. P., and Marti, C. L.: An empirical modeling approach to predict and

- understand phytoplankton dynamics in a reservoir affected by interbasin water transfers, *Water Resour. Res.*, 49, 3626–3641, <https://doi.org/10.1002/wrcr.20268>, 2013.
- Friedman, J. H.: Greedy Function Approximation: A Gradient Boosting Machine, *Ann. Stat.*, 29, 1189–1232, 2001.
- Hanson, P. C., Stillman, A. B., Jia, X., Karpatne, A., Dugan, H. A., Carey, C. C., Stachelek, J., Ward, N. K., Zhang, Y., Read, J. S., and Kumar, V.: Predicting lake surface water phosphorus dynamics using process-guided machine learning, *Ecol. Model.*, 430, 109136, <https://doi.org/10.1016/j.ecolmodel.2020.109136>, 2020.
- Harris, T. D., and Graham, J. L.: Predicting cyanobacterial abundance, microcystin, and geosmin in a eutrophic drinking-water reservoir using a 14-year dataset, *Lake Reserv. Manage.*, 33, 32–48, <https://doi.org/10.1080/10402381.2016.1263694>, 2017.
- Hense, I. and Beckmann, A.: Towards a model of cyanobacteria life cycle – effects of growing and resting stages on bloom formation of  $N_2$ -fixing species, *Ecol. Model.*, 195, 205–218, <https://doi.org/10.1016/j.ecolmodel.2005.11.018>, 2006.
- Hochreiter, S. and Schmidhuber, J.: Long Short-Term Memory, *Neural Comput.*, 9, 1735–1780, <https://doi.org/10.1162/neco.1997.9.8.1735>, 1997.
- Huisman, J., Codd, G. A., Paerl, H. W., Ibelings, B. W., Verspagen, J. M. H., and Visser, P. M.: Cyanobacterial blooms, *Nat. Rev. Microbiol.*, 16, 471–483, <https://doi.org/10.1038/s41579-018-0040-1>, 2018.
- Jia, X., Willard, J., Karpatne, A., Read, J., Zwart, J., Steinbach, M., and Kumar, V.: Physics Guided RNNs for Modeling Dynamical Systems: A Case Study in Simulating Lake Temperature Profiles, in: *Proceedings of the 2019 SIAM* 558–566, <https://doi.org/10.1137/1.9781611975673.63>, 2019.
- Jimeno-Sáez, P., Senent-Aparicio, J., Cecilia, J. M., and Pérez-Sánchez, J.: Using Machine-Learning Algorithms for Eutrophication Modeling: Case Study of Mar Menor Lagoon (Spain), *Int. J. Env. Res. Pub. He.*, 17, 1189, <https://doi.org/10.3390/ijerph17041189>, 2020.
- Jöhnk, K. D., Brüggemann, R., Rücker, J., Luther, B., Simon, U., Nixdorf, B., and Wiedner, C.: Modelling life cycle and population dynamics of Nostocales (cyanobacteria), *Environ. Modell. Softw.*, 26, 669–677, <https://doi.org/10.1016/j.envsoft.2010.11.001>, 2011.
- Karlsson-Elfgren, I., Rengefors, K., and Gustafsson, S.: Factors regulating recruitment from the sediment to the water column in the bloom-forming cyanobacterium *Gloeotrichia echinulata*, *Freshwater Biol.*, 49, 265–273, <https://doi.org/10.1111/j.1365-2427.2004.01182.x>, 2004.
- Karlsson-Elfgren, I., Hyenstrand, P., and Riydin, E.: Pelagic growth and colony division of *Gloeotrichia echinulata* in Lake Erken, *J. Plankton Res.*, 27, 145–151, <https://doi.org/10.1093/plankt/fbh165>, 2005.
- Lin, S.: Shuqi-Lin/Erken\_Algal\_Bloom\_Machine\_Learning\_Model: Erken\_Algal\_Bloom\_Machine\_Learning\_Model (v1.1), Zenodo [code and data set], <https://doi.org/10.5281/zenodo.7149563>, 2022.
- Marcé, R., George, G., Buscarinu, P., Deidda, M., Dunalska, J., de Eyto, E., Flaim, G., Grossart, H.-P., Istvanovics, V., Lenhardt, M., Moreno-Ostos, E., Obrador, B., Ostrovsky, I., Pierson, D. C., Potužák, J., Poikane, S., Rinke, K., Rodríguez-Mozaz, S., Staehr, P. A., Šumberová, K., Waajen, G., Weyhenmeyer, G. A., Weathers, K. C., Zion, M., Ibelings, B. W., and Jennings, E.: Automatic High Frequency Monitoring for Improved Lake and Reservoir Management, *Environ. Sci. Technol.*, 50, 10780–10794, <https://doi.org/10.1021/acs.est.6b01604>, 2016.
- McHugh, M. L.: Interrater reliability: the kappa statistic, *Biochem. Medica*, 22, 276–282, 2012.
- Mellios, N., Moe, S. J., and Laspidou, C.: Machine Learning Approaches for Predicting Health Risk of Cyanobacterial Blooms in Northern European Lakes, *Water*, 12, 1191, <https://doi.org/10.3390/w12041191>, 2020.
- Mesman, J. P., Ayala, A. I., Goyette, S., Kasparian, J., Marcé, R., Markensten, H., Stelzer, J. A. A., Thayne, M. W., Thomas, M. K., Pierson, D. C., and Ibelings, B. W.: Drivers of phytoplankton responses to summer wind events in a stratified lake: A modeling study, *Limnol. Oceanogr.*, 67, 856–873, <https://doi.org/10.1002/lno.12040>, 2022.
- Moras, S., Ayala, A. I., and Pierson, D. C.: Historical modelling of changes in Lake Erken thermal conditions, *Hydrol. Earth Syst. Sci.*, 23, 5001–5016, <https://doi.org/10.5194/hess-23-5001-2019>, 2019.
- Nelson, N. G., Muñoz-Carpena, R., Philips, E. J., Kaplan, D., Sucsy, P., and Hendrickson, J.: Revealing Biotic and Abiotic Controls of Harmful Algal Blooms in a Shallow Subtropical Lake through Statistical Machine Learning, *Environ. Sci. Technol.*, 52, 3527–3535, <https://doi.org/10.1021/acs.est.7b05884>, 2018.
- Paerl, H. W.: Nuisance phytoplankton blooms in coastal, estuarine, and inland waters, *Limnol. Oceanogr.*, 33, 823–843, <https://doi.org/10.4319/lo.1988.33.4part2.0823>, 1988.
- Paerl, H. W. and Huisman, J.: Blooms Like It Hot, *Science*, 320, 57–58, <https://doi.org/10.1126/science.1155398>, 2008.
- Peretyatko, A., Teissier, S., De Backer, S., and Triest, L.: Classification trees as a tool for predicting cyanobacterial blooms, *Hydrobiologia*, 689, 131–146, <https://doi.org/10.1007/s10750-011-0803-4>, 2012.
- Persson, I. and Jones, I. D.: The effect of water colour on lake hydrodynamics: a modelling study, *Freshwater Biol.*, 53, 2345–2355, <https://doi.org/10.1111/j.1365-2427.2008.02049.x>, 2008.
- Pettersson, K.: The Availability of Phosphorus and the Species Composition of the Spring Phytoplankton in Lake Erken, *Internationale Revue der gesamten Hydrobiologie und Hydrographie*, 70, 527–546, <https://doi.org/10.1002/iroh.19850700407>, 1985.
- Pettersson, K.: Mechanisms for internal loading of phosphorus in lakes, *Hydrobiologia*, 373, 21–25, <https://doi.org/10.1023/A:1017011420035>, 1998.
- Pettersson, K., Grust, K., Weyhenmeyer, G., and Blenckner, T.: Seasonality of chlorophyll and nutrients in Lake Erken – effects of weather conditions, *Hydrobiologia*, 506, 75–81, <https://doi.org/10.1023/B:HYDR.0000008582.61851.76>, 2003.
- Pierson, D. C., Pettersson, K., and Istvanovics, V.: Temporal changes in biomass specific photosynthesis during the summer: regulation by environmental factors and the importance of phytoplankton succession, *Hydrobiologia*, 243, 119–135, <https://doi.org/10.1007/BF00007027>, 1992.
- Rahmani, F., Lawson, K., Ouyang, W., Appling, A., Oliver, S., and Shen, C.: Exploring the exceptional performance of a deep learning stream temperature model and the value of streamflow data, *Environ. Res. Lett.*, 16, 024025, <https://doi.org/10.1088/1748-9326/abd501>, 2021.
- Read, J. S., Hamilton, D. P., Jones, I. D., Muraoka, K., Winslow, L. A., Kroiss, R., Wu, C. H., and Gaiser, E.: Derivation

- of lake mixing and stratification indices from high-resolution lake buoy data, *Environ. Modell. Softw.*, 26, 1325–1336, <https://doi.org/10.1016/j.envsoft.2011.05.006>, 2011.
- Read, J. S., Jia, X., Willard, J., Appling, A. P., Zwart, J. A., Oliver, S. K., Karpatne, A., Hansen, G. J. A., Hanson, P. C., Watkins, W., Steinbach, M., and Kumar, V.: Process-Guided Deep Learning Predictions of Lake Water Temperature, *Water Resour. Res.*, 55, 9173–9190, <https://doi.org/10.1029/2019WR024922>, 2019.
- Rousso, B. Z., Bertone, E., Stewart, R., and Hamilton, D. P.: A systematic literature review of forecasting and predictive models for cyanobacteria blooms in freshwater lakes, *Water Res.*, 182, 115959, <https://doi.org/10.1016/j.watres.2020.115959>, 2020.
- Recknagel, F., Fukushima, T., Hanazato, T., Takamura, N., and Wilson, H.: Modelling and prediction of phyto- and zooplankton dynamics in Lake Kasumigaura by artificial neural networks, *Lakes & Reservoirs: Research & Management*, 3, 123–133, <https://doi.org/10.1111/j.1440-1770.1998.tb00039.x>, 1998.
- Reichwaldt, E. S. and Ghadouani, A.: Effects of rainfall patterns on toxic cyanobacterial blooms in a changing climate: Between simplistic scenarios and complex dynamics, *Water Res.*, 46, 1372–1393, <https://doi.org/10.1016/j.watres.2011.11.052>, 2012.
- Richardson, J., Miller, C., Maberly, S. C., Taylor, P., Globevnik, L., Hunter, P., Jeppesen, E., Mischke, U., Moe, S. J., Pasztaleniec, A., Søndergaard, M., and Carvalho, L.: Effects of multiple stressors on cyanobacteria abundance vary with lake type, *Glob. Change Biol.*, 24, 5044–5055, <https://doi.org/10.1111/gcb.14396>, 2018.
- Stanley, F. K. T., Irvine, J. L., Jacques, W. R., Salgia, S. R., Innes, D. G., Winquist, B. D., Torr, D., Brenner, D. R., and Goodarzi, A. A.: Radon exposure is rising steadily within the modern North American residential environment, and is increasingly uniform across seasons, *Scientific Reports*, 9, 18472, <https://doi.org/10.1038/s41598-019-54891-8>, 2019.
- Watson, S. B., Miller, C., Arhonditsis, G., Boyer, G. L., Carmichael, W., Charlton, M. N., Confesor, R., Depew, D. C., Höök, T. O., Ludsins, S. A., Matisoff, G., McElmurry, S. P., Murray, M. W., Peter Richards, R., Rao, Y. R., Steffen, M. M., and Wilhelm, S. W.: The re-eutrophication of Lake Erie: Harmful algal blooms and hypoxia, *Harmful Algae*, 56, 44–66, <https://doi.org/10.1016/j.hal.2016.04.010>, 2016.
- Wei, B., Sugiura, N., and Maekawa, T.: Use of artificial neural network in the prediction of algal blooms, *Water Res.*, 35, 2022–2028, [https://doi.org/10.1016/S0043-1354\(00\)00464-4](https://doi.org/10.1016/S0043-1354(00)00464-4), 2001.
- Xiao, X., He, J., Huang, H., Miller, T. R., Christakos, G., Reichwaldt, E. S., Ghadouani, A., Lin, S., Xu, X., and Shi, J.: A novel single-parameter approach for forecasting algal blooms, *Water Res.*, 108, 222–231, <https://doi.org/10.1016/j.watres.2016.10.076>, 2017.
- Yang, Y., Stenger-Kovács, C., Padisák, J., and Pettersson, K.: Effects of winter severity on spring phytoplankton development in a temperate lake (Lake Erken, Sweden), *Hydrobiologia*, 780, 47–57, <https://doi.org/10.1007/s10750-016-2777-8>, 2016.